Super-resolved Microscopy

DOI: 10.1002/anie.201410265

Super-resolved Fluorescence Microscopy: Nobel Prize in Chemistry 2014 for Eric Betzig, Stefan Hell, and William E. Moerner**

*Leonhard Möckl, Don C. Lamb, and Christoph Bräuchle**

Nobel Prize · PALM · single molecule detection · STED · super-resolution

The Nobel Prize in Chemistry 2014 was jointly awarded to Eric Betzig, Stefan Hell, and William E. Moerner "*for the development of super-resolved fluorescence microscopy*". Nearly 150 years ago, Ernst Abbe formulated his famous equation for the best resolution achievable with optical microscopy, which was believed to be impossible to overcome:

$$\Delta x_{\min}, \Delta y_{\min} = \lambda/(2n\sin\alpha) \approx \lambda/2$$

where λ is the wavelength of the light, n the index of refraction of the microscopy medium and α half the aperture angle of the objective lens.[1] This implies that objects separated by less than 200 nm, that is, about half of the wavelength used, cannot be resolved by light microscopy. It was the groundbreaking work of the three Nobel laureates that showed ways to circumvent this limit and transferred optical microscopy into nanoscopy. With super-resolved fluorescence microscopy, scientists are now capable of following the pathway of an individual molecule inside a living cell, observing molecules as they create synapses between nerve cells in the brain, and resolving the aggregation of proteins involved in Parkinson's, Alzheimer's, and Huntington's diseases, to mention only few of the new challenges mastered.[2] How did all this come about?

The Nobel laureates developed two different and independent approaches for circumventing the resolution limit and achieving super resolution. One approach uses the detection of single molecules and their precise localization down to few nanometers[3] (Moerner 1989) and a strategy[4] to precisely localize many single molecules that define a complex structure (Betzig 1995/2006). The other approach employs patterned illumination to spatially control the emission of excited fluorophores[5] (Hell 1994/2000). We first describe the single-molecule-based approach and continue with the patterned illumination technique.

In 1952, Erwin Schrödinger wrote: "*[…] we never experiment with just one electron or atom or (small) molecule. In thought-experiments we sometimes assume that we do;*"[6] Within less than four decades, W. E. Moerner[3] showed this statement to be false when, in 1989, he was able to detect the absorption of a single molecule. One year later, Michel Orrit was able to detect a single molecule using fluorescence.[7] Whereas these approaches were performed at cryogenic temperatures,[8] the first detection of single molecules in solution at ambient temperatures, which is especially important for biology, was also published in 1990.[9] Together, these experiments laid the cornerstone for the development of single molecule spectroscopy and microscopy, inspiring numerous research approaches that brought the concept of single molecules to physics, chemistry, and biology.[10] Up until this point, ensemble averaging of the molecular behavior was limiting the direct observation of what molecules were really doing. Among the numerous new insights created by single molecule detection, its application in microcopy was the most influential.

Although the intensity profile of a single fluorescent emitter is subject to diffraction, its center can be localized with much higher precision: Whereas the size of an emitter molecule is about 1 nm, the fluorescent spot produced by diffraction within the microscope is actually about 200 nm. Figures 1a and 1b show the intensity profile of such a diffraction-limited signal referred to as the point spread function

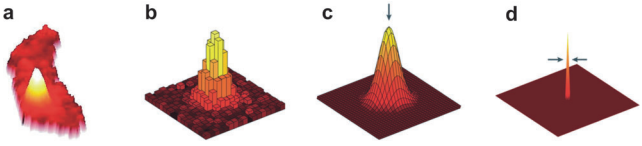

Figure 1. Diffraction-limited detection and localization accuracy. When photons are detected from a single emitter, they form a diffraction-limited pattern called the PSF. a) The original PSF of a single YFP molecule in a bacteria cell; b) the pixelated PSF measured on the camera; c) a two-dimensional Gaussian fit to the PSF; d) the high-precision localization of the emitter determined from the center of the PSF.[35]

[*] M. Sc. L. Möckl, Prof. Dr. D. C. Lamb, Prof. Dr. C. Bräuchle
Department for Chemistry and Center for NanoScience (CeNS)
University of Munich (LMU)
Butenandtstrasse 5–13 (E), 81377 Munich (Germany)
E-mail: Christoph.Braeuchle@lmu.de

[**] We gratefully acknowledge the assistance of Frauke Mickler and Philipp Messer.

(PSF), which can be approximated by a two-dimensional Gaussian function (Figure 1c). Provided the detected signal is generated by only one emitter (that is, a single molecule), the center of the PSF determines the position of the emitter with very high accuracy (often called super localization). As the number of photons detected from a single emitter increases, the accuracy with which the peak position of the PSF can be determined improves and the position of a single emitter can be localized more precisely. Hence, Abbe's formula can be modified to incorporate the enhanced localization precision:

$$\Delta x_{\min}, \Delta y_{\min} = [\lambda/(2n \sin \alpha)]/\sqrt{N}$$

where N is the total number of photons detected. Thus for example, with 100 detected photons, the resolution for the localization of a single emitter is increased by a factor of 10 (Figure 1d). This high-resolution microscopy paved the way for tracking single molecules with nanometer localization accuracy (FIONA, 1.5 nm), unraveling for example the hand-over-hand movement of the motor protein Myosin V[11] or the three-dimensional movement of mRNA particles in yeast cells.[12]

Whereas one emitter is sufficient for single-molecule tracking, microscopy of complex structures needs many emitters (labels) to visualize their features correctly (Figure 2a). However, when all the labels are excited simultaneously (Figure 2b), high-precision localization of the individual emitters is no longer possible due to overlapping of the PSFs, leading to a blurred or non-resolved image. This is what is measured in a conventional optical fluorescence microscope. Unfortunately, sparse or diluted labeling of the structures, resulting in separated PSFs, is not sufficient for imaging the structure correctly owing to undersampling of the image as described by the Nyquist–Shannon criterion.[13] In other words, a high concentration of emitters is needed to resolve the features of the structure correctly while, at the same time, a low concentration is needed to separate the PSFs of the individual emitters for performing high-precision localization microscopy.

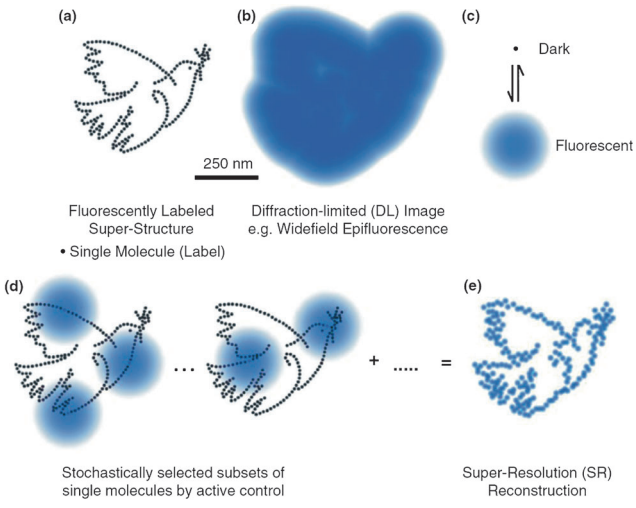

Figure 2. The principle of localization microscopy. a) An arrangement of fluorescent molecules representing La Paloma de la Paz (P. Picasso, 1961) with a spatial frequency below that of the diffraction limit. b) Were this structure to be visualized by conventional microscopy, Abbe's criterion forbids resolution of the individual features. c,d) However, by stochastically switching molecules between a fluorescent state and a dark state, the PSF of a few sparse emitters can be acquired in each acquisition step. Their positions are determined with high precision and (e), in a pointillist approach, the results of all localizations are combined to obtain a super-resolved reconstruction of the object.[36]

It was Eric Betzig who first made a valuable suggestion[4a] for a solution to this contradiction. His idea was to isolate the emitters by some spectral property. The separated subsets of emitters each form a sparse set in space. Thus, the position of the emitters within one subset can be determined with high accuracy. By sequentially measuring all the subsets, a super-resolution image can be generated by combining all the high-precision localizations. At that time, the optical property Betzig suggested for separating the individual subsets was the inhomogeneity in the absorption wavelength.[14] However, this turned out to be difficult to realize.

It was once more W. E. Moerner who, after getting the ball rolling, contributed to an alternate solution. When he investigated mutants of the green fluorescent protein (GFP), he encountered a strange photophysical behavior of the T203F mutant.[15] The mutant fluoresced when illuminated with 488 nm light and eventually switched into a non-fluorescent dark state. Amazingly, it was not irreversibly photobleached but could be reactivated by 405 nm illumination (Figure 2c). This finding triggered the search for other GFP mutants with similar photophysical switching characteristics, although they were not originally designed with subdiffractive microscopy in mind.[16]

It again took Betzig, returning to university after some years of working in industry, to "connect the dots" and make the final step towards super-resolution microscopy. He recognized that such photoactivable (pa) fluorescent proteins are capable of solving the problem of sparse and dense labeling in the following way: The sample is labeled densely with paGFP molecules that are in a dark state at the beginning of the experiment. With a low-powered laser pulse having the appropriate wavelength, a few fluorescent proteins are stochastically transferred to the active state so that they form a sparse subset. They are subsequently visualized by 488 nm excitation in a single-molecule manner until they completely photobleach. After photobleaching, new fluorescent proteins are activated in the following frames and the cycle starts over again (Figure 2d). Finally, one obtains the full, complex picture in high resolution by summing up all the highly resolved single emitters of each frame (Figure 2e). The tremendous gain in resolution is best visualized by two images taken from Betzig's 2006 landmark publication[4b] where he introduced the technique as Photo-Activated Localization Microscopy or PALM with a resolution of typically about 20 nm (Figure 3).

In summary, two key elements are required to create a super-resolution image of a complex structure by localization microscopy. First, the fluorophores labeling the structure must be actively controllable in such a way that in every image frame only a sparse subset of labels are emitting

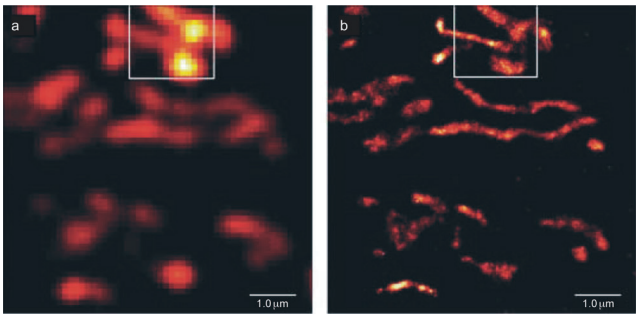

Figure 3. Super-resolved images of mitochondria in COS-7 cells. a) A total internal reflection fluorescence (TIRF) microscopy image and b) the PALM super-resolution image of mitochondria in COS-7 cells. The mitochondria were labeled using a photoactivable fluorescent protein (dEosFP) targeted to the matrix of the mitochondria. Whereas only the approximate shape of the mitochondria can be resolved using TIRF microscopy, PALM microscopy exhibits features on the length scale of about 20 nm, well below the diffraction limit.[4b]

and that their diffraction-limited signals are thus spatially well-separated. Second, each diffraction-limited PSF of a single molecule has to be fitted with an appropriate model function to estimate the position of the emitter with high precision. The collection of molecular positions determined with high accuracy allows then the reconstruction of the structure in a pointillist fashion. Besides PALM, two other ways of producing super-resolved images by localization microscopy using different actively controlled fluorophore switching mechanisms were introduced in 2006: fPALM,[17] and STORM.[18] In the meantime, numerous sophisticated approaches using actively controlled fluorophore switching mechanisms have been developed.[2]

However, there are also limitations to be overcome. One is that high-quality super-resolution images need a lot of individual localizations, limiting the overall time resolution. Moreover, image reconstruction needs time-consuming post processing. Furthermore, life does not take place in two dimensions, but is three-dimensional. Numerous new schemes have been developed to account for this. Among others, astigmatism-[19] and double-helix PSF-based imaging[20] were introduced to provide super-resolution localization in the z-dimension. Additional advances include multicolor imaging[21] and faster data collection and analysis methods for video-rate imaging.[22]

An alternate approach for super-resolved imaging based on patterned illumination was developed by Stefan Hell. Finding ways to enhance the resolution of the optical microscope was a goal of Stefan Hell since early in his scientific career. While at the University of Turku in Finland, he published a paper in 1994 discussing a theoretical approach for obtaining optical images below the diffraction limit, STimuated Emission Depletion (STED) Microscopy.[5a] In this approach, one laser beam is used to excite the sample, as in traditional confocal microscopy. The excitation beam is subject to diffraction, just as we already described for the fluorescence emission, and hence has its own PSF. A second, patterned laser beam deexcites molecules that are not centered in the excitation PSF (Figure 4a). Deexcitation is induced by stimulated emission, one of the fundamental interactions of light with matter along with absorption and spontaneous emission (Figure 4b). The molecules at the center of the excitation PSF are unaffected by the STED beam and still fluoresce. Thus, the effective size of the excitation PSF is reduced (Figure 4a, right panel).

After publication of his idea, many microscopists were skeptical that the concept would really work. However, Stefan Hell received a chance to realize STED microscopy when the Max Planck Institute in Göttingen, Germany, offered him a junior group leader position in December 1996. The first realization of STED microscopy came in 2000,[5b] when the STED beam was used to increase the axial resolution of the microscope by over a factor 5 from a full-width half-maximum of 490 nm down to 97 nm (Figure 4c, bottom panel). Since the initial STED experiment, elegant ways have also been developed to significantly increase the radial resolution[23] and both approaches have been combined to enhance the resolution in all three dimensions.[24]

There are three important aspects that need to be combined in STED microscopy. The first aspect is the use of stimulated emission to return molecules to the ground state. The focus of the STED beam is overlapped with the excitation laser beam such that molecules outside the very center of the excitation beam PSF are switched back to the ground state via stimulated emission. The second important aspect for STED microscopy is engineering the pattern of the STED beam at the sample so that there is zero intensity at its center. Thus, fluorophores at the very center of the excitation PSF remain in the excited state and can fluoresce. This is currently achieved using phase plates that generate constructive and destructive interference to create the desired illumination pattern of the STED beam (for example a toroid or "donut"). The third important aspect of STED microscopy is the ability to saturate the transition that switches off the fluorophore (Figure 4d). Therefore, the final resolution depends upon the physical properties of the fluorophore and the intensity of the STED beam. The resolution achievable with STED can be expressed by modifying Abbe's equation:

$$\Delta x_{\min}, \Delta y_{\min} = \lambda / \left[(2n \sin \alpha) \sqrt{1 + I_{\mathrm{STED}}/I_{\mathrm{sat}}} \right]$$

where I_{STED} is the intensity of the STED beam and I_{sat} is related to the probability of a molecule undergoing stimulated emission by the STED beam and depends on the molecular properties of the fluorophore. An example that clearly demonstrates the power of STED is shown in Figure 4e. The transmembrane synaptic-vesicle protein, synaptotagmin I, in purified endosomes was labeled and imaged using confocal and STED microscopy.[25] The high resolution achievable with STED allows visualization of small protein clusters within endosomes.

The charm of STED is that it physically reduces the effective PSF of the microscope and can be used with a large ensemble of molecules and with single molecules. However, STED also has its limitations. The most sever limitation is the high laser power needed for stimulated emission. This can

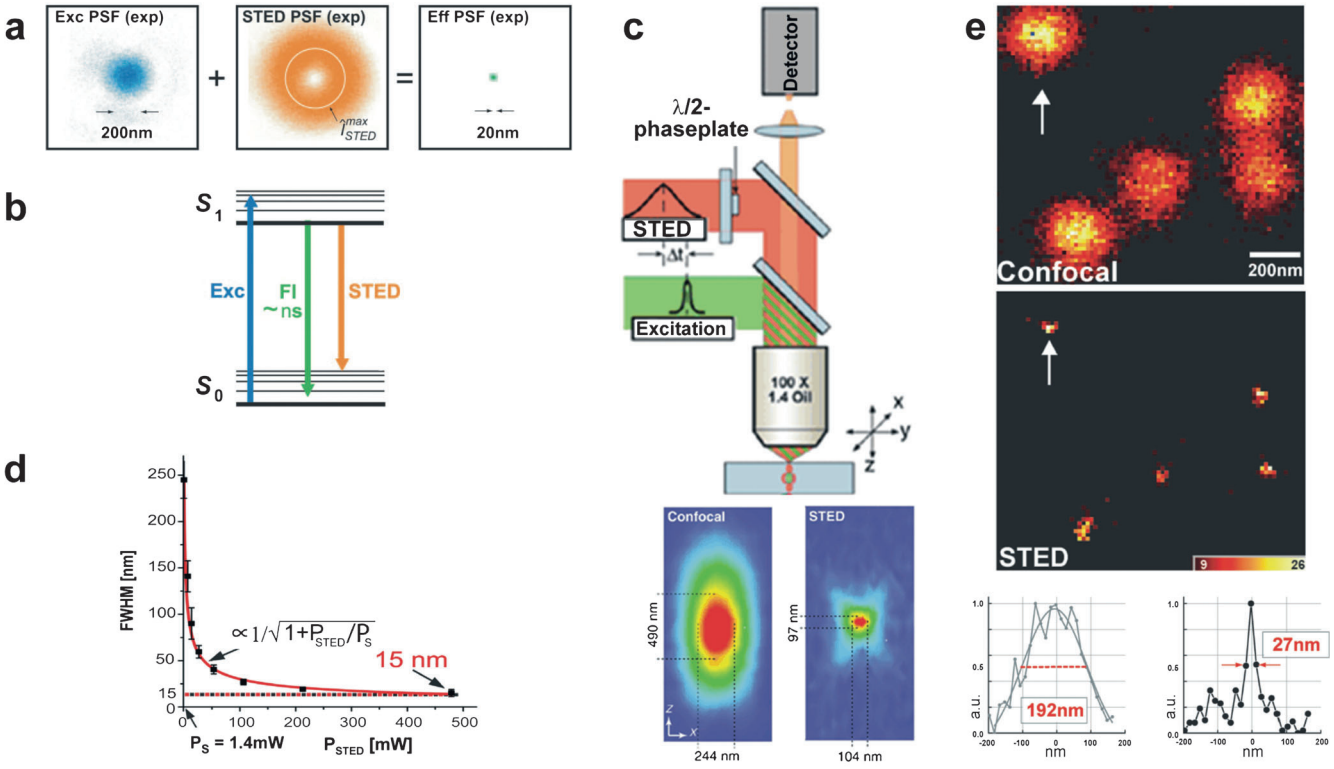

Figure 4. The principles of STED microscopy. a) Measured profiles of the excitation beam (left), the STED beam (center) and the effective PSF (right).[25] b) A Jablonski diagram showing the basic transitions occurring in STED microscopy. Fluorophores are excited to the S1 state using the excitation laser. The STED laser deexcites molecules outside the center of the PSF from the ground vibrational state of the excited state to a high vibrational state of the ground state. The emitted light is blocked at the detector with proper filters. Molecules at the center of the PSF return to the ground state via fluorescence and are detected with an effectively reduced PSF.[25] c) Upper: the first realized STED microscope. Lower: the PSF from 48 nm beads labeled with the fluorophore LDS 751 measured using confocal microscopy and with STED microscopy. In the STED image, the lateral size of the PSF was reduced from 490 nm to 97 nm.[5b] d) The full-width half-maximum (FWHM) of the effective PSF as a function of the intensity of the STED beam.[33] e) Synaptotagmin I molecules within endosomes. The confocal image (top) shows diffraction-limited spots with a size around 200 nm. The STED microscope image (center) reveals the true size of the spots to be around 30 nm. Bottom: Intensity profiles of the endosomes highlighted with arrows in the upper panel, demonstrating the dramatic increase in optical resolution.[25]

lead to significant photobleaching of the sample and can be a concern when measuring in live cells. Furthermore, the fluorophores needed for STED microscopy have to be photostable, which limits the choice of fluorophores.

Nevertheless, STED microscopy is evolving rapidly, with new capabilities or enhancements being regularly developed. For example, two- and three-color STED microscopy has been realized,[26] new fluorophores are being developed,[27] the resolution further increased by using the fluorescence lifetime information,[28] and STED has been combined with fluorescence correlation spectroscopy[29] to investigate lipid rafts, to name only a few. Recently, a related method, referred to as RESOFLT,[30] has been developed based on photoswitchable proteins to perform super-resolution imaging in a STED-like fashion but at laser intensities of about one-millionth of that used for traditional STED microscopy.

Importantly, the power of super-resolution microscopy is not only its high resolution: electron microscopes, for example, outperform any optical method. Nevertheless, combining super resolution with the specificity of fluorescent labels and the possibility of imaging cells easily without complicated sample preparation makes experiments possible with super-resolution optical microscopy that cannot be performed using any other technique. Furthermore, it allows dynamical processes to be followed in living cells, which is not possible with electron microscopy. Four examples of recent findings employing super-resolution microscopy techniques are given in Figure 5. They demonstrate the influence of super-resolution microscopy in various fields: Chromosome segregation in bacteria,[31] huntingtin aggregation in neurons,[32] the architecture of the nuclear pore complex,[33] and in vivo imaging of dendrites inside a living mouse brain.[34]

Single-molecule experiments and super-resolved imaging have already been embraced by the scientific community. Furthermore, experimental setups for these methods are commercially available, making it accessible to non-specialists. Thus, the stage is set for the broad application of these methods ranging from chemistry and cell biology to medicine.

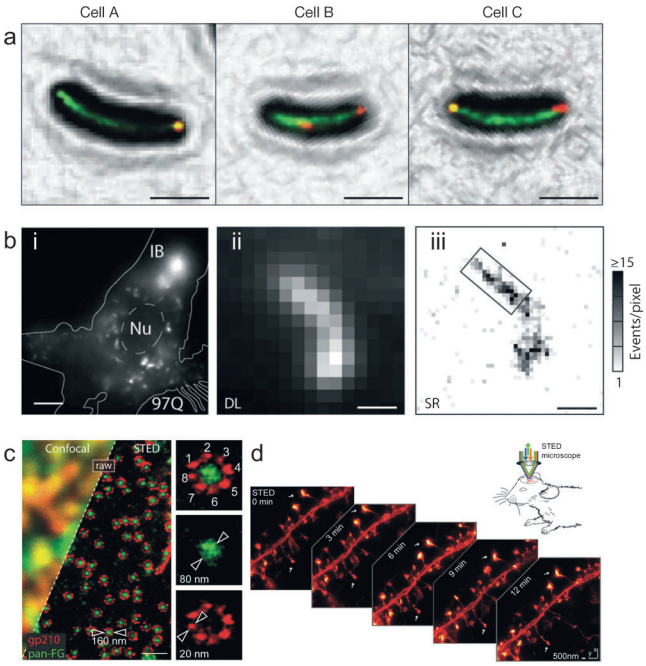

Figure 5. Recent examples of super-resolution imaging in living cells. a) The partitioning (Par) apparatus for chromosome segregation in *Caulobacter crescentus* was imaged using dual-color PALM. Discrete linear assemblies of the ATPase ParA are resolved that guide the ParB-parS complex towards the new pole (green: ParA-eYFP, red: ParB-CFP). Three cells are shown at different stages of cell division: Cell A: before replication initiation, Cell B: during segregation, Cell C: after completion of parS segregation (scale bar: 1 μm).[31] b) Small huntingtin aggregates in neuronal model cells (PC12 m). i,ii) Diffraction-limited images showing the subcellular distribution of mutant huntingtin exon 1 proteins (Htt1-ex1-97Q-eYFP; 16 h post transfection). Nu = nucleus, scale bar = 5 μm for (i) and 500 nm for (ii). iii) Super-resolution (SR) reconstruction by PALM of an individual small huntingtin aggregate shown in panel (ii) (scale bar: 500 nm). The boxed region was analyzed to determine the thickness of the fiber (about 90 nm).[32] This is the first time that small huntingtin aggregates were observed, which are thought to be the disease-relevant species. c) A dual-color STED image of amphibian nuclear pore complexes (NPCs). The upper left-hand region of the images is shown with confocal resolution for comparison. The eight-fold symmetry of the outer ring of the NPCs was visualized using specific antibodies against gp210 (shown in red). In a second color, the center of the NPC was visualized using antibodies specific for labeling the nucleoporins (shown in green). Scale bar: 500 nm.[33] d) STED microscopy of actin in neuron cells of living mice using YFP-lifeact. Dynamic rearrangement of the actin in dendritic spines over the course of 12 min is shown with a resolution of about 60 nm.[34]

With super-resolution fluorescence microscopy being so interdisciplinary, involving optical resolution, which is a physical problem, and important applications in biology, one may ask why the Nobel Prize was awarded in Chemistry. However, molecules are at the center of these methods, and the main results concern molecules, molecular structures, and their behavior.

Received: October 20, 2014
Published online: November 4, 2014

[1] E. Abbe, *Arch. Mikrosk. Anat. Entwicklungsmech.* **1873**, *9*, 413 – 418.
[2] M. A. Thompson, M. D. Lew, W. E. Moerner, *Annu. Rev. Biophys.* **2012**, *41*, 321 – 342.
[3] W. E. Moerner, L. Kador, *Phys. Rev. Lett.* **1989**, *62*, 2535 – 2538.
[4] a) E. Betzig, *Opt. Lett.* **1995**, *20*, 237 – 239; b) E. Betzig, G. H. Patterson, R. Sougrat, O. W. Lindwasser, S. Olenych, J. S. Bonifacino, M. W. Davidson, J. Lippincott-Schwartz, H. F. Hess, *Science* **2006**, *313*, 1642 – 1645.
[5] a) S. W. Hell, J. Wichmann, *Opt. Lett.* **1994**, *19*, 780 – 782; b) T. A. Klar, S. Jakobs, M. Dyba, A. Egner, S. W. Hell, *Proc. Natl. Acad. Sci. USA* **2000**, *97*, 8206 – 8210; c) S. W. Hell, M. Kroug, *Appl. Phys. B* **1995**, *60*, 495 – 497.
[6] E. Schrödinger, *Br. J. Phil. Sci.* **1952**, *III*, 233 – 242.
[7] M. Orrit, J. Bernard, *Phys. Rev. Lett.* **1990**, *65*, 2716 – 2719.
[8] W. E. Moerner, T. Basché, *Angew. Chem. Int. Ed. Engl.* **1993**, *32*, 457 – 476; *Angew. Chem.* **1993**, *105*, 537 – 557.
[9] E. B. Shera, N. K. Seitzinger, L. M. Davis, R. A. Keller, S. A. Soper, *Chem. Phys. Lett.* **1990**, *174*, 553 – 557.
[10] *Single Molecule Spectroscopy in Chemistry, Physics and Biology, (Nobel Symposium 2008)* (Hrsg.: A. Gräslund, R. Rigler, J. Widenrgen), Springer, Heidelberg, **2010**.
[11] A. Yildiz, J. N. Forkey, S. A. McKinney, T. Ha, Y. E. Goldman, P. R. Selvin, *Science* **2003**, *300*, 2061 – 2065.
[12] M. A. Thompson, J. M. Casolari, M. Badieirostami, P. O. Brown, W. E. Moerner, *Proc. Natl. Acad. Sci. USA* **2010**, *107*, 17864 – 17871.
[13] a) C. E. Shannon, *Proc. IRE* **1949**, *37*, 10 – 21; b) H. Nyquist, *Trans. AIEE* **1928**, *47*, 617 – 644.
[14] A. M. van Oijen, J. Kohler, J. Schmidt, M. Muller, G. J. Brakenhoff, *Chem. Phys. Lett.* **1998**, *292*.
[15] R. M. Dickson, A. B. Cubitt, R. Y. Tsien, W. E. Moerner, *Nature* **1997**, *388*, 355 – 358.
[16] G. H. Patterson, J. Lippincott-Schwartz, *Science* **2002**, *297*, 1873 – 1877.
[17] S. T. Hess, T. P. Girirajan, M. D. Mason, *Biophys. J.* **2006**, *91*, 4258 – 4272.
[18] M. J. Rust, M. Bates, X. Zhuang, *Nat. Methods* **2006**, *3*, 793 – 795.
[19] B. Huang, W. Wang, M. Bates, X. Zhuang, *Science* **2008**, *319*, 810 – 813.
[20] S. R. Pavani, M. A. Thompson, J. S. Biteen, S. J. Lord, N. Liu, R. J. Twieg, R. Piestun, W. E. Moerner, *Proc. Natl. Acad. Sci. USA* **2009**, *106*, 2995 – 2999.
[21] H. Shroff, C. G. Galbraith, J. A. Galbraith, H. White, J. Gillette, S. Olenych, M. W. Davidson, E. Betzig, *Proc. Natl. Acad. Sci. USA* **2007**, *104*, 20308 – 20313.
[22] F. Huang, T. M. Hartwich, F. E. Rivera-Molina, Y. Lin, W. C. Duim, J. J. Long, P. D. Uchil, J. R. Myers, M. A. Baird, W. Mothes, M. W. Davidson, D. Toomre, J. Bewersdorf, *Nat. Methods* **2013**, *10*, 653 – 658.
[23] P. Török, P. R. T. Munro, *Opt. Express* **2004**, *12*, 3605 – 3617.
[24] D. Wildanger, R. Medda, L. Kastrup, S. W. Hell, *J. Microsc.* **2009**, *236*, 35 – 43.
[25] G. Donnert, J. Keller, R. Medda, M. A. Andrei, S. O. Rizzoli, R. Luhrmann, R. Jahn, C. Eggeling, S. W. Hell, *Proc. Natl. Acad. Sci. USA* **2006**, *103*, 11440 – 11445.
[26] a) G. Donnert, J. Keller, C. A. Wurm, S. O. Rizzoli, V. Westphal, A. Schonle, R. Jahn, S. Jakobs, C. Eggeling, S. W. Hell, *Biophys. J.* **2007**, *92*, L67 – 69; b) J. Bückers, D. Wildanger, G. Vicidomini, L. Kastrup, S. W. Hell, *Opt. Express* **2011**, *19*, 3130 – 3143.
[27] V. N. Belov, G. Y. Mitronova, M. L. Bossi, V. P. Boyarskiy, E. Hebisch, C. Geisler, K. Kolmakov, C. A. Wurm, K. I. Willig, S. W. Hell, *Chem. Eur. J.* **2014**, *20*, 13162—13173.
[28] a) J. R. Moffitt, C. Osseforth, J. Michaelis, *Opt. Express* **2011**, *19*, 4242 – 4254; b) G. Vicidomini, G. Moneron, K. Y. Han, V.

Westphal, H. Ta, M. Reuss, J. Engelhardt, C. Eggeling, S. W. Hell, *Nat. Methods* **2011**, *8*, 571 – 573.
[29] C. Eggeling, C. Ringemann, R. Medda, G. Schwarzmann, K. Sandhoff, S. Polyakova, V. N. Belov, B. Hein, C. von Middendorff, A. Schonle, S. W. Hell, *Nature* **2009**, *457*, 1159 – 1162.
[30] T. Grotjohann, I. Testa, M. Leutenegger, H. Bock, N. T. Urban, F. Lavoie-Cardinal, K. I. Willig, C. Eggeling, S. Jakobs, S. W. Hell, *Nature* **2011**, *478*, 204 – 208.
[31] J. L. Ptacin, S. F. Lee, E. C. Garner, E. Toro, M. Eckart, L. R. Comolli, W. E. Moerner, L. Shapiro, *Nat. Cell Biol.* **2010**, *12*, 791 – 798.
[32] S. J. Sahl, L. E. Weiss, W. C. Duim, J. Frydman, W. E. Moerner, *Sci. Rep.* **2012**, *2*, 895.
[33] F. Göttfert, C. A. Wurm, V. Mueller, S. Berning, V. C. Cordes, A. Honigmann, S. W. Hell, *Biophys. J.* **2013**, *105*, pL01 – L03.
[34] K. I. Willig, H. Steffens, C. Gregor, A. Herholt, M. J. Rossner, S. W. Hell, *Biophys. J.* **2014**, *106*, L01 – 03.
[35] a) A. Gahlmann, W. E. Moerner, *Nat. Rev. Microbiol.* **2014**, *12*, 9 – 22; b) W. E. Moerner, *Proc. Natl. Acad. Sci. USA* **2007**, *104*, 12596 – 12602.
[36] S. J. Sahl, W. E. Moerner, *Curr. Opin. Struct. Biol.* **2013**, *23*, 778 – 787.